Nuclear Science
2017; 2(2): 44-53
http://www.sciencepublishinggroup.com/j/ns
doi: 10.11648/j.ns.20170202.13

Mineralogical and Radiological Micro-Analysis of Raw Sands and Their Processed By-Products for Land Reclamation Applications

Osama A. M. Ebyan[1], Mahmoud R Khattab[1, *], Mohamed A. E. Abdel-Rahman[2]

[1]Nuclear Materials Authority (NMA), El-Maadi, Cairo, Egypt

[2]Nuclear Engineering Department, Military Technical College, Kobry El-Kobba, Cairo, Egypt

Email address:

MahmoudkhattabNMA@yahoo.com (M. R. Khattab)

[*]Corresponding author

To cite this article:

Osama A. M. Ebyan, Mahmoud R Khattab, Mohamed A. E. Abdel-Rahman. Mineralogical and Radiological Micro-Analysis of Raw Sands and Their Processed By-Products for Land Reclamation Applications. *Nuclear Science.* Vol. 2, No. 2, 2017, pp. 44-53.
doi: 10.11648/j.ns.20170202.13

Received: February 3, 2017; **Accepted**: February 23, 2017; **Published**: March 15, 2017

Abstract: In this study, forty samples of different types of raw sands, magnetite, green silicate and processed mixture of ilmenite, magnetite and green silicates have been mineralogical and radiometrically investigated after preparation. Determination of the mineral contents, radioactivity levels and their corresponding environmental impacts was also carried out. The radioactivity: ^{238}U, ^{232}Th, ^{226}Ra and ^{40}K, of these samples are of naturally occurring origin. The EDX analysis was applied for identification of trace elements in the samples. The microscopic investigations of the samples indicate that the black sand samples are economically rich in heavy minerals such as ilmenite, magnetite, zircon, rutile and monazite; in addition to leucoxene. While the processed and unprocessed green silicate contain ilmenite, zircon, sphene, monazite and calamine with quartz and other silicate minerals. The highest values of activity concentrations of ^{238}U, ^{232}Th, ^{226}Ra and ^{40}K were observed in black sand, processed and unprocessed green silicates samples. These high radioactivities are attributed to the presence of zircon, monazite and sphene. The radiological hazard parameters; the absorbed dose rate (D), annual effective dose equivalent AEDE, radium equivalent activity Ra_{eq}, external hazard index H_{ex}, internal hazard index H_{in} and gamma activity concentration index Iγ of the studied samples were estimated. The results obtained were tabulated, evaluated, interpreted and discussed.

Keywords: Mineralogical, Radioactivity Levels, Radiological Hazards Assessment, Raw Sand, Black Sand, Green Silicate, Environmental Impact, Land Reclamation

1. Introduction

The Egyptian black sand deposits extend along the Mediterranean coast from Abu Qir in the west to Rafah in the east (Figure 1). Most of the deposits are present either as beach sediment or sand dune [1]. The importance of the black sand deposits is their generation potentials from their contents of many strategic and economic minerals as ilmenite, magnetite, zircon, monazite, rutile, leucoxene and garnet together with trace minerals such as native gold, thorite and cassiterite [2, 3]. Many studies were carried out on the Egyptian black sands since half of the last century, concerning mineralogy, evaluation and upgrading of these economic heavy minerals [4, 5, 6, 7, 8, 9, 10, 11, 12 and 13]. The Egyptian black sands contain several economic minerals, such as ilmenite, magnetite, garnet, zircon, rutile and monazite.

In the present work, raw sands were collected from the topmost meter from the area containing black spots of black sand. Using both wet-gravity concentration, high-tension electrostatic separation and both low- and high-intensity magnetic separation techniques, most of the individual economic mineral concentrates were obtained with marketable grades and acceptable recoveries [9, 14, 15, 16, 5 and 6].

Prepared samples from black sand byproducts and some of its original products were used by some companies for desert reclamation. These prepared samples are mainly composed of mixture from black sand byproducts in addition to some

isolated products. Sample mixtures include in most cases, green silicate minerals, magnetite and ilmenite with percentages reach up to 65%, 25% and 10%, respectively. This mixture can be used for the reclamation of desert soil, where it contains some important elements that improve soil properties and also used as mineral Fertilizers.

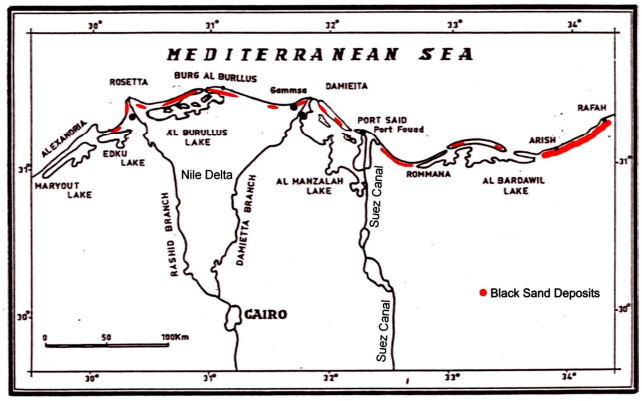

Figure 1. *Location map of the black sand resources on the Mediterranean Coast.*

U and Th are long-lived radionuclides with a suite of radioactive daughter products which can pose a human-health and ecological risk. Radiation of natural origin is responsible for most of the total radiation exposure to the general population. Quantification of background levels of radionuclides is necessary to evaluate the potential environmental risk, to determine the boundary of areas of high natural background and to establish its cleanup level [17, 18 and 19]. The study of the concentrations and distributions of the natural radionuclides in the processed Egyptian black sand, its main constituents and byproducts allows the understanding of the radiological implication of these elements due to the gamma ray exposure of the body and irradiation of lung tissue from inhalation of radon and its daughters. In particular, it is also important to assess the radiation hazards arising due to the use of processed black sand products and byproducts in desert reclamation.

2. Analytical Methods

The collected samples were subjected to different physical ore dressing techniques include gravity Wilfley shaking table and magnetic low and high intensity magnetic separators tools. Firstly, each dry field sample was subjected to sieving over a 2.0 mm screen to remove shell and rock fragments and any other plant remnants to facilitate the different concentration methods (Figure 2).

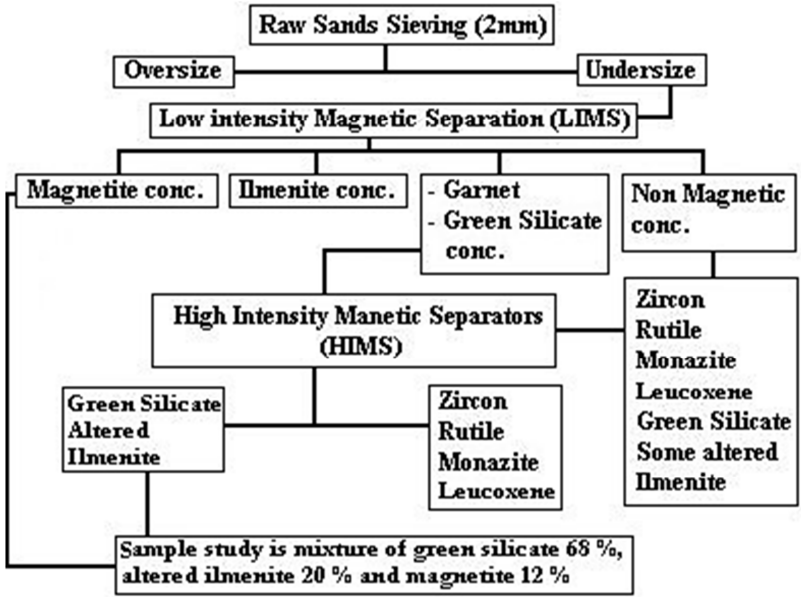

Figure 2. *Simplified flow sheet showing the various concentration and separation steps for different components and by-products of the studied black sand (modified after Moustafa 2010 [1]).*

The separation was done by the Wilfley shaking tables for wet gravity concentration. The Carpco high–tension roll-type electrostatic separator–model HP-167 and model Hp-114 was used for high tension electrostatic separation and the Carpco magnetic separator, model–MLH (13) 111-5 for magnetic separation. High-purity concentrate of individual economic minerals are obtained by using wet-gravity concentration, high-tension electrostatic separation and both low and high intensity magnetic separation at the optimum adjustments of operating conditions [9].

The significant difference in specific gravities between gangue minerals such as quartz (2.65) and green silicate minerals (3.5, in average) and the economic minerals such as monazite (5.2), ilmenite (4.7), zircon (4.6), rutile (4.2), garnet (4.0) and magnetite (4.9) has been utilized.

The difference in the magnetic susceptibilities between economic minerals has also been utilized. The bulk of the economic minerals concentrate is separated into two major fractions, namely; magnetic and non-magnetic. Each of these two major fractions has been further classified according to

their electrical conductivity. The conductor rutile is separated from the nonconductor zircon and the conductor ilmenite is separated from the nonconductor garnet using the high tension electrostatic separation. Most of associated fine green silicate and quartz grains are removed in a tailing fraction. Most of the contaminated trace monazite grains, cassiterite and gold are included in the top strip tabled fraction in association with relatively finer rutile grains [20].

To identify the common mineral constituents of the beach sands and green silicates, 10 samples were selected and prepared for mineralogical study. Each sample was quartered several times to obtain a representative sample of about 120 g. The samples were sieved using +2 mm sieve to remove trash materials. Then, the samples were subjected to heavy liquid separation technique using bromoform solution (sp. gr. 2.81 g/cm^3). The heavy fractions resulted from the heavy liquid separation were magnetically fractionated by using a permanent hand magnet to collect magnetite grains from the samples. Then the magnetite-free samples were magnetically fractionated by using Frantz Isodynamic Magnetic Separator (Model L1) at 0.2, 0.5 and 1 current amperes. A suitable quotient was taken and studied under a binocular stereomicroscope. Semi-quantitative EDX chemical analyses were performed by a XL30 Phillips Type Environmental Scanning Electron Microscope (ESEM).

3. Results and Discussion

3.1. Mineralogical Investigations

Mineralogical studies of the investigated black sand and green silicate samples indicate that black sand samples are mainly composed of ilmenite, zircon, rutile, sphene and monazite while processed green silicate contains ilmenite, zircon, sphene, monazite and calamine in addition to quartz and other silicate minerals.

Zircon ($ZrSiO_4$): Zircon occurs predominantly as euhedral to subhedral grains in fine to very fine sizes. They are commonly prismatic to elongated grains of good adamantine luster. Some of the prismatic zircons are characterized by bipyramidal termination (Figure 3A, B & Figure 4 A). The oval, needle, spherical and fragments are also presents. The majority of zircon grains exhibit transparent, rarely translucent, colourless to pale yellow colours. Some of zircon grains exhibit different colour shades from yellow, yellowish red to brown colours.

Monazite-(Ce): The importance of monazite raises because of its content of the light rare earth elements (REE), Th and U [21, 22, 23, and 13]. Monazite mineral grains in the studied stream sediments are generally subhedral, sometimes euhedral, flattened or broken grains occasionally exhibit pitted surfaces (Figure 3C & Figure 4D). Monazite is light to deep canary and lemon yellow colors. Yellowish red to brown monazite grains are rarely found. Moustafa M. I (2009) [10] reported that the change in monazite color is attributed to the content of Ce_2O_3 as well as Th, U and Ca. They are round to well- round transparent mineral grains with resinous luster. EDX chemical analyses of some monazite grains confirm that these monazites to be monazite-(Ce) with Ce as the dominant REE.

Apatite: It occurs in scarce amounts in most studied samples and this may be related to rarity in the source rocks. Apatite included within monazite occurs as elongated crystals (Figure 3D).

Rutile (TiO_2): Rutile is the preferred mineral for the production of titanium dioxide. Rutile mineral grains are subhedral to anhedral grains in fine to very fine sizes. The majority of them have prismatitic, tabular and elongated forms. Fragmental and irregular rutile grains are frequently observed. Rutile colors vary widely from yellowish red, red, reddish brown, brown to black exhibiting adamantine luster. Variation in color is due to the impurity ions occupied the crystal internal structure, especially the ferric iron, niobium and tantalum [20]. The EDX chemical analyses of some rutile mineral grains illustrate rutile grains are characterized by relatively high titanium content (Figure 3E).

Calamine ($Zn_4Si_2O_7(OH)_2 \cdot H_2O$) is the original name of the mineral Hemimorphite, and described this zinc ore in globular and botryoidal forms. The mineral Smithsonite, which closely resembles Hemimorphite and is also a zinc ore, was also called Calamine by the miners and early collectors. The so-called «Calamine» ores consist of a supergene mixture of zinc carbonates and hydroxyl-carbonates and silicates. The «Calamine» ores are considered to be the result of the in situ oxidation of primary carbonate-hosted sulfide ores, and subsequent remobilisation and redeposition as internal sediments into dissolution vugs and karst cavities [26]. It is pale blue, spiky crystals. EDAX analyses indicate that this mineral is mainly composed of zinc (Figure 3F).

Leucoxene: Leucoxene generally is developed from the alteration of Ilmenite, where it contains more than 70% of TiO_2. In the leucoxenation process the Ilmenite structure is destroyed and iron ions migrate outside [24]. It is the transitional phase during the alteration of Ilmenite to the Secondary rutile. It is characterized by rough-pitted surface. Leucoxene is present as fine, rounded grains. The color of leucoxene grains varies from dark brown, pale brown, creamy to grey colors (Figure 3G).

Magnetite (Fe_3O_4): Magnetite has the inverse spinel structure. It occurs naturally as solid solution with many spinel components [25]. It occurs in the studied samples as angular to subangular, fine grains. They range in their color from dull black to brownish black and assume metallic to submetallic luster (Figure 3H).

Ilmenite ($Fe\text{-}TiO_3$): Ilmenite is the most abundant Fe-Ti oxide mineral that occurs in a wide variety of igneous rocks, some metamorphic rocks and as detrital mineral grains. It is the dominant economic minerals in the studied black sand deposits in the studied samples. Ilmenite mineral grains are confined to medium to fine sand size fraction. They exhibit iron-black to brownish black colors with metallic to sub-metallic luster. The bulk of Ilmenite grains are irregular in shape. Some of them exhibit rhombohedral form. The obtained data from EDX chemical analysis reveal that the

major components are Titanium and iron (Figure 4B).

Sphene (Ca Ti [SiO] (O, OH, F): Sphene exhibits prismatic, tabular and platy crystals. The colour of sphene ranges from yellowish brown to brown colours. It is translucent mineral crystals with resinous luster. The semi-quantitative analysis (EDX) shows the chemical composition of sphene (Figure 4C).

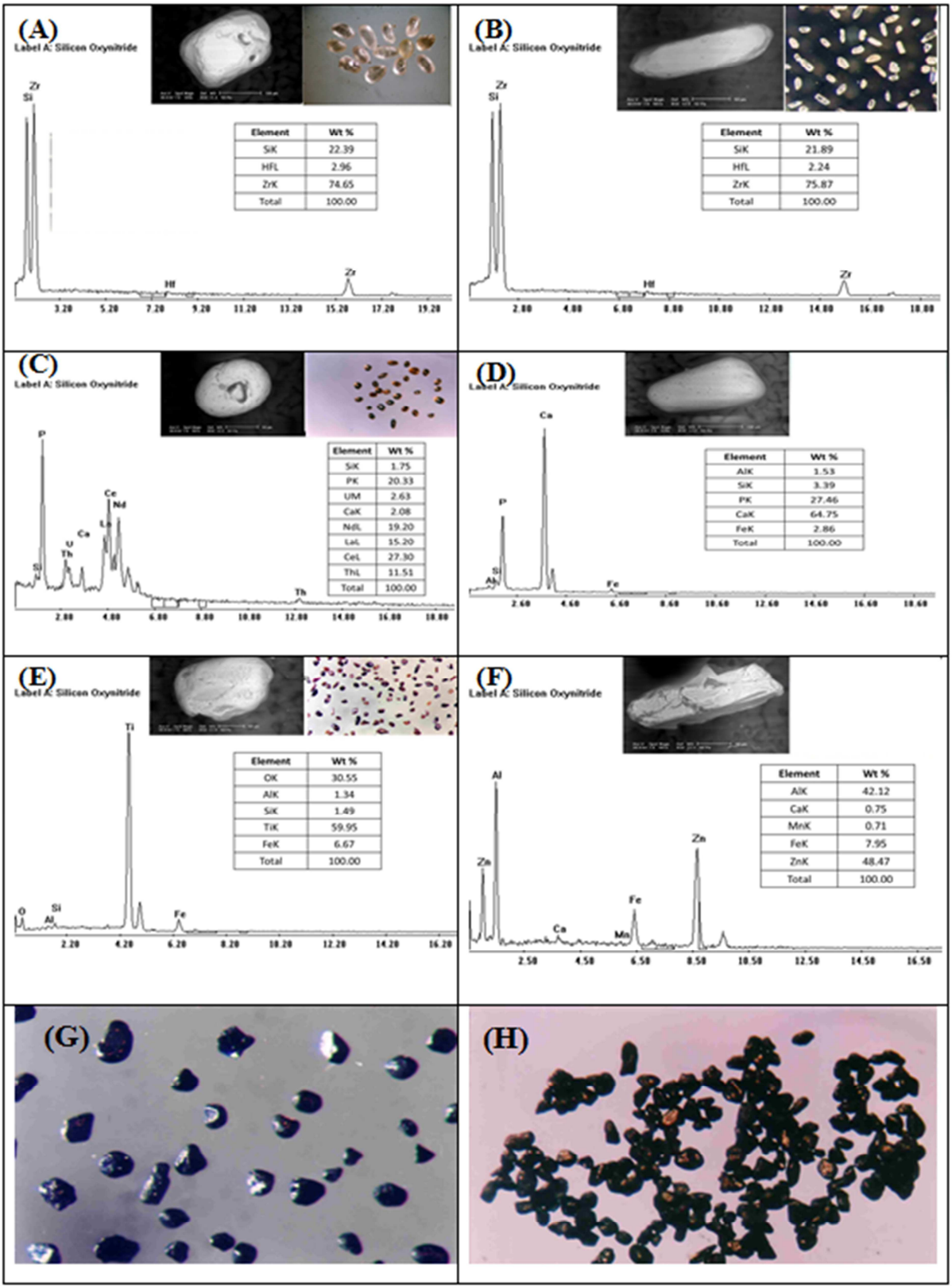

Figure 3. *EDX mineral analyses, SEM images and photomicrograph of economic heavy minerals in the studied black sands. A and B Zircon; C. Monazite; D. Apatite; E. Rutile; F. Calamine G. Leucoxene; H. Magnetite.*

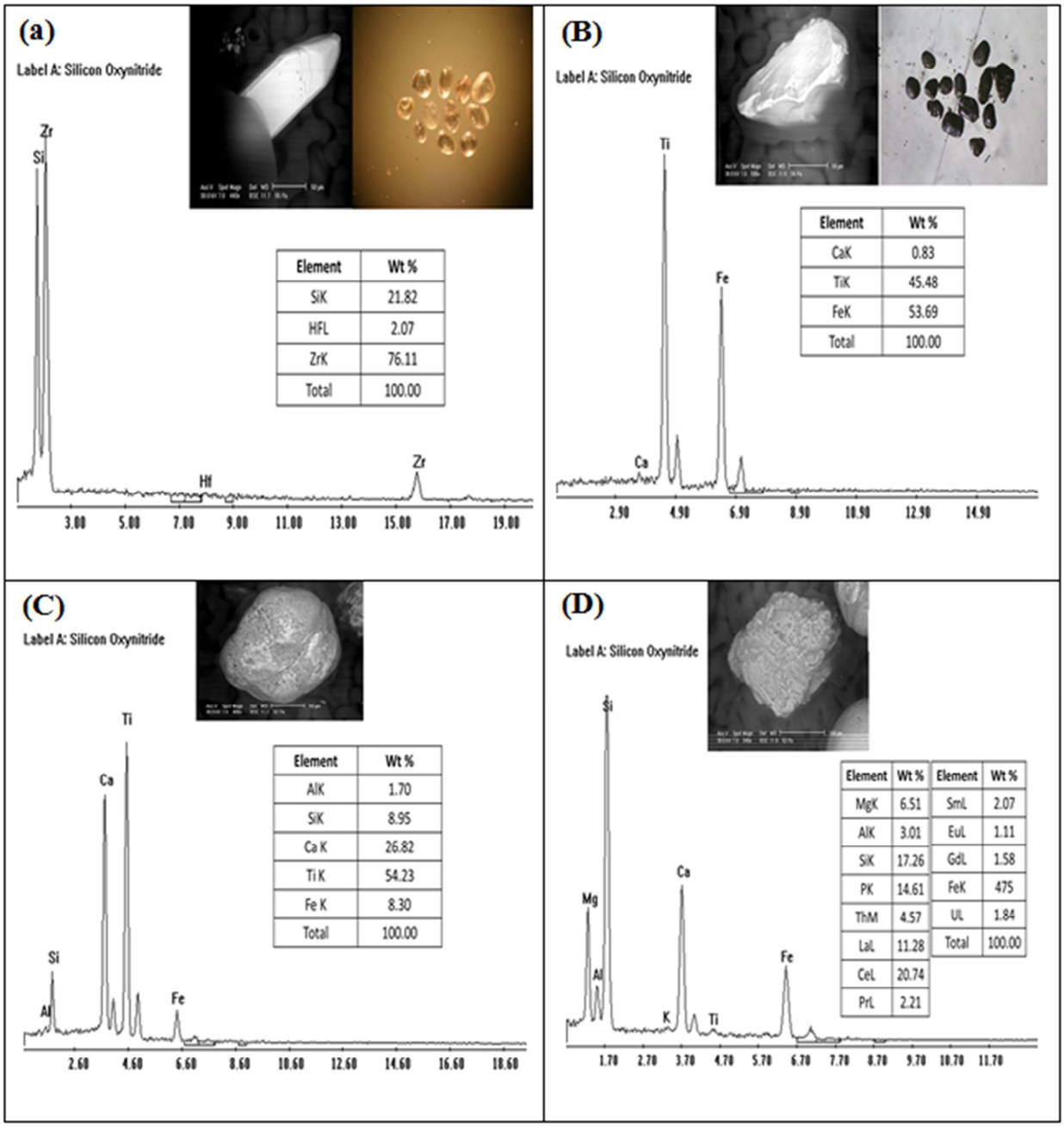

Figure 4. *EDX mineral analyses, SEM images and photomicrograph of the most common economic heavy minerals of the studied processed green silicate samples. a. Zircon; b. Ilmenite; c. Sphene; d. Monazite.*

3.2. Distribution of Radionuclides

Measurements of radioelements concentration for Uranium (eU), Thorium (eTh), Radium (Ra) (eU) and Potasium (K) were determined for forty samples in the studied sediments and expressed in ppm (as shown in tables 1-4). From the tables, eU, eTh, Ra (eU) and K concentrations in black sand samples varied from 1.48 to 2.10 ppm with average value 1.75±0.23 ppm, from 180 to 258 with average value 220.3±21 ppm, from 29 to 34 with average value 32.19±1.8 ppm and from 0.09 to 0.13 with average value 0.11±0.011%, respectively. In case of unprocessed green silicate, radioelements concentration range from 1 to 10 with average value 5.9±2.8 ppm, from 43 to 52 ppm with average value 48±2.94 ppm, from 12 to 15 with average value 13.6±0.84 ppm and from 0.05 to 0.16% with average value 0.11±0.04%, respectively. For magnetite, the radioelements concentration showed a change from 1.1 to 2.1 with average value 1.6±0.32 ppm, from 7 to 10 with average value 8.10±0.99 ppm, from 1 to 2 with average value 1.1±0.31 ppm and from 0.02 to 0.06 with average value 0.05±0.015%, respectively. As for processed green silicate, radioelements concentration varied from 1.47 to 2 with average value 1.72±0.21 ppm, from 24 to 29 with average value 26.7±1.63 ppm, from 5 to 50 with average value 5.5±0.52 ppm and from 0.01 to 0.2 with average value 0.12±0.07%, respectively.

3.3. Absorbed Dose Rate and Relative Values

Values of eU and eTh in ppm, as well as K, in %, were converted to activity concentration, in Bq/kg, using the conversion factors given by International Atomic Energy Agency, [26] and by Polish Central Laboratory for Radiological Protection [27, 28]. The specific parent activity of a sample containing 1 ppm, by weight, of U is 12.35 Bq/kg, 1 ppm of Ra is 11.1 Bq/kg, and 1 ppm of Th is 4.06 Bq/kg, and 1% of ^{40}K is 313 Bq/ kg. Therefore it can be easy to estimate the effects of this radiation through the calculation of the following parameters.

a. Absorbed Dose Rate in Air (D)

The absorbed gamma dose rate (D in nGy/hr) in air at 1m above the ground surface for the uniform distribution of radionuclides (^{226}Ra, ^{232}Th and ^{40}K) were calculated by using Eq.(1) on the basis of guide lines provided by UNSCEAR (2000) [30] and Örgün et al., (2007) [31].

$$D\ (nGy\ h^{-1}) = 0.462A_U + 0.604A_{Th} + 0.0417A_K \quad (1)$$

where A_U, A_{Th} and A_K are the average specific activities of ^{238}U, ^{232}Th and ^{40}K in Bq/kg, respectively in the measured samples.

The average absorbed γ- dose rate (D) values for black sand, magnetite, green silicate and prepared mixed samples are shown in tables 1-4. The values obtained in black sand ranged between 450.2 and 640.1 nGyh^{-1} with an average 548.9±51.27 nGyh^{-1}, for magnetite between 25.3 and 34.1 with average 29.5±2.44 nGyh^{-1}, for green silicate between 128.4 and 185.8 with 152.3±18.5 nGyh^{-1} as an average and for prepared mixed samples between 68.1 and 82.9 with average 76.5±4.4 nGyh^{-1} as an average. The high average values of the studied black sand, green silicate and prepared mixed samples (548.9±51.27, 152.3±18.5 and 76.5±4.4 nGyh^{-1} respectively), which is higher than the world average value 57 nGyh^{-1} [32, 33], could be due to these samples have a high activity concentration values, particularly based on radionuclides of ^{232}Th. These values are consistent with previous reports [31, 32] by Tzortzis et al. and Örgün et al.

Table 1. *Results of radionuclide concentrations, the absorbed dose rate (D), the annual effective dose equivalent (AEDE), radium equivalent activity (Ra_{eq}), external (H_{ex}), internal (H_{in}) hazard indices and gamma index (I_γ) of black sand samples (BS).*

Sample No	eU ppm	eTh ppm	Ra ppm	K (%)	eU Bq/Kg	eTh Bq/Kg	Ra Bq/Kg	K Bq/Kg	D (nGy/hr)	AEDE (mSv/y)	Raeq (Bq/Kg)	Hex	Hin	Iγ
Bs1	1.5	220	32	0.09	18.53	888.8	355.2	28.17	546.60	0.670	1627.0	3.48	3.53	9.03
Bs2	1.6	210	29	0.12	19.76	848.4	321.9	37.56	523.16	0.641	1536.7	3.33	3.39	8.64
Bs3	1.48	221	34	0.13	18.28	892.84	377.4	40.69	549.45	0.673	1656.0	3.50	3.55	9.07
Bs4	1.6	258	33	0.11	19.79	1042.3	366.3	34.43	640.16	0.785	1857.9	4.08	4.13	10.57
Bs5	2.1	227	33	0.1	25.94	917.08	366.3	31.3	567.25	0.695	1678.8	3.61	3.68	9.36
Bs6	1.99	208	30	0.1	24.6	840.32	333	30.98	520.24	0.638	1535.8	3.31	3.38	8.58
Bs7	1.89	208	31	0.1	23.35	840.32	344.1	30.67	519.65	0.637	1546.9	3.31	3.37	8.57
Bs8	2	238	34	0.11	24.7	961.52	377.4	34.43	593.65	0.728	1753.6	3.78	3.85	9.80
Bs9	1.7	180	31	0.1	21	727.2	344.1	30.04	450.22	0.552	1385.2	2.87	2.92	7.43
Bs10	1.6	233	34	0.1	19.77	941.32	377.4	30.67	579.00	0.710	1724.5	3.69	3.74	9.56
Min	1.48	180	29.00	0.09	18.28	727.20	321.90	28.17	450.22	0.55	1385.20	2.87	2.92	7.43
Max	2.10	258	34.00	0.13	25.94	1042.30	377.40	40.69	640.16	0.79	1857.90	4.08	4.13	10.57
Av. ±SD	1.75 ±0.23	220.30 ±21	32.10 ±1.8	0.11 ±0.011	21.58 ±2.81	890.01 ±84.9	356.31 ±19.9	32.89 ±3.85	548.94 ±51.27	0.67 ±0.063	1630.24 ±134.84	3.50 ±0.33	3.55 ±0.32	9.06 ±0.85

Table 2. *Results of radionuclide concentrations, the absorbed dose rate (D), the annual effective dose equivalent (AEDE), radium equivalent activity (Raeq), external (Hex), internal (Hin) hazard indices and gamma index (Iγ) for unprocessed green Silicate samples (GS).*

Sample No	eU ppm	eTh ppm	Ra ppm	K (%)	eU Bq/Kg	eTh Bq/Kg	Ra Bq/Kg	K Bq/Kg	D (nGy/hr)	AEDE (mSv/y)	Ra_{eq} (Bq/Kg)	H_{ex}	H_{in}	I_γ
Gs1	7	43	13	0.06	86.8	173.7	144.3	21.28	145.91	0.178	394.1	0.91	1.14	2.33
Gs2	6	46	14	0.05	74.4	185.8	155.4	18.46	147.39	0.180	422.3	0.92	1.12	2.37
Gs3	8	51	12	0.06	99.2	206.0	133.2	18.78	171.06	0.209	429	1.07	1.34	2.73
Gs4	8	48	14	0.16	99.2	193.9	155.4	50.08	165.04	0.202	436.3	1.03	1.3	2.63
Gs5	3	45	14	0.11	37.2	181.8	155.4	34.43	128.43	0.157	417.8	0.81	0.91	2.09
Gs6	8	47	15	0.12	99.2	189.9	166.5	37.56	162.08	0.198	440.6	1.01	1.28	2.58
Gs7	4	51	13	0.14	49.6	206.0	144.3	43.82	149.19	0.182	442	0.94	1.07	2.42
Gs8	10	52	13	0.13	124	210.1	144.3	40.69	185.87	0.227	447.5	1.15	1.49	2.95
Gs9	1	50	14	0.14	12.4	202.0	155.4	43.82	129.56	0.158	447.3	0.82	0.86	2.13
Gs10	4	47	14	0.09	49.6	189.8	155.4	30.98	138.89	0.170	429	0.87	1.01	2.25
Min	1	43	12	0.05	12.4	173.7	133.2	18.46	128.43	0.16	394.10	0.81	0.86	2.09
Max	10	52	15	0.16	124	210.10	166.5	50.08	185.87	0.23	447.50	1.15	1.49	2.95
Av. ±SD	5.90 ±2.8	48 ±2.94	13.6 ±0.84	0.11 ±0.039	73.16 ±34	193.90 ±11.9	150.96 ±9.36	33.99 ±11.3	152.34 ±18.5	0.19 ±0.022	430.59 ±16.32	0.95 ±0.11	1.15 ±0.2	2.45 ±0.27

Table 3. *Results of radionuclide concentrations, the absorbed dose rate (D), the annual effective dose uivalent (AEDE), radium equivalent activity (Ra_{eq}), external (H_{ex}), internal (H_{in}) hazard indices and gamma index (I_γ) for magnetite samples (M).*

Sample No	eU ppm	eTh ppm	Ra ppm	K (%)	eU Bq/Kg	eTh Bq/Kg	Ra Bq/Kg	K Bq/Kg	D (nGy/hr)	AEDE (mSv/y)	Ra_{eq} (Bq/Kg)	H_{ex}	H_{in}	I_γ
M1	1.4	8	1	0.04	17.36	32.32	11.1	12.52	28.06	0.034	58.2	0.17	0.2	0.45
M2	1.3	9	1	0.02	16.12	36.36	11.1	6.26	29.67	0.036	63.5	0.19	0.2	0.47
M3	1.1	9	1	0.06	13.64	36.36	11.1	18.78	29.05	0.035	64.5	0.18	0.2	0.46
M4	1.33	7	1	0.05	16.49	28.28	11.1	15.65	25.35	0.031	52.7	0.16	0.2	0.40
M5	2.1	8	1	0.06	26.04	32.32	11.1	18.78	32.33	0.039	58.7	0.2	0.3	0.51
M6	1.99	7	2	0.03	24.68	28.28	22.2	9.39	28.87	0.035	63.3	0.18	0.2	0.45
M7	1.85	8	1	0.03	22.94	32.32	11.1	9.39	30.51	0.037	58	0.19	0.3	0.48
M8	1.6	10	1	0.04	19.84	40.4	11.1	13.15	34.11	0.041	69.8	0.21	0.3	0.54
M9	1.7	7	1	0.06	21.08	28.28	11.1	20.03	27.65	0.033	53	0.17	0.2	0.43
M10	1.68	8	1	0.06	20.83	32.32	11.1	18.47	29.91	0.037	58.7	0.18	0.2	0.47
Min	1.10	7	1	0.02	13.64	28.28	11.10	6.26	25.35	0.03	52.70	0.16	0.20	0.40
Max	2.10	10	2	0.06	26.04	40.40	22.20	20.03	34.11	0.04	69.80	0.21	0.30	0.54
Av. ±SD	1.61 ±0.32	8.10 ±0.99	1.10 ±0.31	0.05 ±0.015	19.90 ±3.99	32.72 ±4.02	12.21 ±3.51	14.24 ±4.82	29.55 ±2.44	0.036 ±0.003	60.04 ±5.3	0.18 ±0.015	0.23 ±0.048	0.47 ±0.04

Table 4. *Results of radionuclide concentrations, the absorbed dose rate (D), the annual effective dose equivalent (AEDE), radium equivalent activity (Ra_{eq}), external (H_{ex}), internal (H_{in}) hazard indices and gamma index (I_γ) for processed green silicate samples (IMG).*

Sample No	eU ppm	eTh ppm	Ra ppm	K (%)	eU Bq/Kg	eTh Bq/Kg	Ra Bq/Kg	K Bq/Kg	D (nGy/hr)	AEDE (mSv/y)	Ra_{eq} (Bq/Kg)	H_{ex}	H_{in}	I_γ
IMG1	1.5	28	5	0.01	18.6	113.12	55.5	3.13	77.04	0.09	217.34	0.49	0.54	1.25
IMG2	2.0	25	6	0.05	24.8	101.0	66.6	15.65	73.11	0.09	212.09	0.46	0.52	1.18
IMG3	1.6	24	6	0.03	19.84	96.96	66.6	9.39	68.12	0.08	205.83	0.429	0.48	1.10
IMG4	1.65	28	6	0.09	20.46	113.12	66.6	30.98	79.07	0.09	230.58	0.50	0.55	1.29
IMG5	1.84	25	6	0.08	22.81	101.0	66.6	26.60	72.65	0.09	212.93	0.46	0.52	1.18
IMG6	1.95	27	5	0.11	24.18	109.08	55.5	34.43	78.49	0.09	213.97	0.49	0.56	1.27
IMG7	1.65	29	5	0.21	20.46	117.16	55.5	65.73	82.96	0.10	227.92	0.52	0.57	1.35
IMG8	2.0	27	5	0.19	24.8	109.08	55.5	59.47	79.82	0.09	215.90	0.50	0.57	1.29
IMG9	1.54	26	5	0.18	19.09	105.04	55.5	56.34	74.61	0.09	209.89	0.47	0.52	1.21
IMG10	1.47	28	6	0.21	18.22	113.12	66.6	65.73	79.48	0.09	233.25	0.50	0.55	1.29
Min	1.47	24	5	0.01	18.22	96.96	55.5	3.13	68.12	0.08	205.83	0.43	0.48	1.1
Max	2	29	50	0.21	24.8	117.16	66.6	65.73	82.96	0.1	233.25	0.52	0.57	1.35
Av. ±SD	1.72 ±0.21	26.7 ±1.63	5.5 ±0.52	0.116 ±0.076	21.33 ±2.59	107.87 ±6.61	61.05 ±5.85	36.75 ±23.67	76.54 ±4.4	0.09 ±0.0047	217.97 ±9.34	0.48 ±0.026	0.54 ±0.028	1.241 ±0.07

b. Annual Effective Dose Equivalent (AEDE)

The annual effective dose equivalent (AEDE) was calculated from the absorbed dose rate (D) by applying the dose conversion factor of 0.7 Sv/Gy and the outdoor occupancy factor of 0.2 by using the following formula [30, 31]:

$$\text{AEDE (mSv/yr)} = D\ \text{(nGy/hr)} \times 0.7 \times 0.2 \times 8.54 \times 10^{-3} \quad (2)$$

Furthermore, the average values of AEDE for black sand, magnetite, green silicate and prepared mixed samples were also listed (as shown in tables 1-4). The obtained values varied between 0.55 and 0.79 $mSvy^{-1}$ with mean value 0.67±0.063 for black sand samples, between 0.031 and 0.04 with 0.036±0.003 as an average value for magnetite, between 0.16 and 0.23 with 0.17±0.022 $mSvy^{-1}$ as an average value for green silicate and finally for prepared mixed samples varied between 0.08 and 0.1 with 0.09±0.0047 $mSvy^{-1}$ as an average. As for magnetite, green silicate and prepared mixed samples the AEDE values were found to be less than 0.48 $mSvy^{-1}$, which recommended by UNSCEAR (2000) [30] as the worldwide average of the AEDE. In contrast, black sand samples showed the highest values among all samples, higher than the average range of worldwide mean range, which could be attributed to their high thorium activity concentration as mentioned before.

c. Radium equivalent activity, Ra_{eq}

The radium equivalent activity (Ra_{eq}) is a weighted sum of activities of the ^{238}U, ^{232}Th and ^{40}K radionuclides based on the assumption that 370 Bq/ kg of ^{238}U, 259 Bq/ kg of ^{232}Th and 4810 Bq/ kg of ^{40}K produce the same gamma ray dose rate [34].

$$Ra_{eq} = A_U + 1.43\ A_{Th} + 0.077\ A_K \quad (3)$$

Raeq was estimated for the collected rocks and are given in Tables 1-4 for all types of samples.

The values of Raeq varied from 1385.2 to 1857.9 with average value 1630.2±134.84 Bq/kg for black sand, from 52.7 to 69.8 with average value 60±5.3 Bq/kg for magnetite,

from 394.1 to 447.5 with average value 430.5±16.32 Bq/kg for green silicate and finally for prepared mixed samples from 205.8 to 233.2 with 217.9±9.34 as an average. The obtained results are much higher than the acceptable worldwide mean value (less than 370 Bq/kg) for both black sand and green silicate samples. As for magnetite and prepared mixed samples the Raeq is satisfactory as per the recommendations i.e. 60±5.3 and 217.9±9.34.

d. Hazard indices (H_{ex} and H_{in})

1). External hazard index, H_{ex}

The external hazard index (H_{ex}) used to measure the external hazard due to the emitted gamma radiation. It was calculated by using the following equation [34, 31, and 35]:

$$H_{ex} = A_U/370 + A_{Th}/259 + A_K/4810 \leq 1 \quad (4)$$

The external hazard index is obtained from Raeq expression through the supposition that its maximum value allowed (equal to unity) corresponds to the upper limit of Ra_{eq} (370 Bq/kg). For the maximum value of H_{ex} to be less than unity, the maximum value of Ra_{eq} must be less than 370 $Bqkg^{-1}$.

The obtained values of H_{ex} ranged from 2.87 to 4.08 with average value 3.5±0.33 for black sand, from 0.16 to 0.21 with average value 0.18±0.015 for magnetite, from 0.81 to 1.15 with average value 0.95±0.11 for green silicates and finally from 0.42 to 0.52 with an average 0.48±0.026 for prepared mixed samples. The results of external hazard index revealed that their values for the black sand samples (i.e. 3.5±0.33) and some of green silicate samples are higher than the acceptable value, which recommended by IAEA, i.e. $H_{ex}<1$. While for magnetite and prepared mixed samples the H_{ex} is satisfactory as recommended (less than 1). The values range ~0.18±0.015 and 0.48±0.026, respectively. This is due to the relatively low values of the activity concentration of naturally occurring radioactive nuclides.

2). Internal hazard index, H_{in}

The internal hazard index (H_{in}) is used to control the internal exposure to ^{222}Rn and its radioactive progeny. It is given by the following equation [31, 34 and 35]:

$$H_{in} = A_U/185 + A_{Th}/259 + A_K/4810 \leq 1 \quad (5)$$

If the maximum concentration of uranium in samples under investigation is half that of the normal acceptable limit, then the value of H_{in} will be less than 1 [34]. The obtained values of H_{in} were ranged from 2.92 to 4.13 with average value 3.55±0.32 for black sand, from 0.2 to 0.3 with average value 0.23±0.048 for magnetite, from 0.86 to 1.49 with average value 1.15±0.2 for green silicate, and from 0.48 to 0.57 with average value 0.54±0.028 for prepared mixed sample.

It should be noted that there is a significant difference in H_{in} for the four types of samples. In case of black sand and green silicate samples an elevated H_{in} (i.e. 3.55±0.32 and 1.15±0.2, respectively) higher than the acceptable values, was observed. This is due to their high activity concentrations of gamma rays emitted from daughter nuclides of both uranium and thorium. As for magnetite and prepared mixed samples the H_{in} is satisfactory as recommended (less than 1). The values are ~0.23±0.048 and 0.54±0.028 respectively.

e. Gamma activity index, Iγ

The restriction on building materials for gamma radiation is based on a dose range from 0.3 to 1 mSv/y [32]. In order to examine whether a building material meets these limits of dose criteria, the gamma activity concentration index Iγ was calculated from the following equation [32]:

$$I\gamma = \frac{A_U}{300} + \frac{A_{Th}}{200} + \frac{A_K}{3000} \quad (6)$$

The above equation based on the fact that, radionuclides contribute to external irradiation according to the ratios of their specific exposure rate constants, i.e., ^{40}K: ^{238}U: ^{232}Th = 1:10:15. This method uses the sum of three specific activity quotients as an index of gamma irradiation with denominators chosen to reflect the specific exposure rate and yield a sum equal to unity. For the activity concentration index, $I\gamma \leq 2$ corresponds to a dose criterion of 0.3 mSv y^{-1}, while $I\gamma \leq 6$ corresponds to a dose of 1 mSv y^{-1} as reported in the European Commission in 1999 [32, 36]. According to this dose criterion, materials with $I\gamma \geq 6$ should be avoided [37], whereas these values correspond to dose rates higher than 1 mSv/y [38], which is the maximum dose rate value in air recommended for population [30, 39].

The obtained values of Iγ ranged from 7.43 to 10.57 with average value 9.06 ±0.85 for black sand, from 0.4 to 0.54 with average value 0.47±0.04 for magnetite, from 2.09 to 2.95 with average value 2.45±0.27 for green silicate and finally from 1.1 to 1.35 with average value 1.24±0.07 for prepared mixed samples. According to these reults, the average values of Iγ for black sand samples are higher than the acceptable limit ($I\gamma > 6$) which corresponds to dose rates higher than 1 mSv/y [38]. With respect to magnetite, green silicate and prepared mixed sample, it is clear that their values show $2 \leq I\gamma \leq 6$ which indicates gamma dose contribution from these samples exceed 0.3 mSv/y however still lower than the maximum dose rate value in air ($I\gamma < 1$ mSv/y) recommend for population for a safe radiation hazard.

4. Conclusions

It was observed that the maximum radioelements concentration of ^{238}U, ^{232}Th, ^{226}Ra and. K were 2.10 ppm, 258 ppm, 34 ppm and 0.13% for black sand and 10 ppm, 52 ppm, 15 ppm and 0.16-0.11% for unprocessed green silicate, respectively. While, the minimum concentrations were 1.10 ppm, 7 ppm, 1 ppm and 0.02% for magnetite, 1.47 ppm, 24 ppm, 5 ppm and from 0.01%, for processed green silicate, respectively. Based on the results obtained, it can be concluded that the highest ^{238}U, ^{232}Th, ^{226}Ra and ^{40}K values were found in black sand and unprocessed green silicate samples. This is mainly attributed to the presence of zircon, monazite and sphene in these samples. The radiological parameters of the analyzed samples; the dose rate (D), annual

effective dose equivalent (AEDE), radium equivalent activity (Ra_{eq}), external hazard index (H_{ex}), internal hazard index (H_{in}) and gamma activity concentration index (I_{γ}) was calculated and evaluated. Fairly, it was observed that many of the investigated samples from black sand, processed and unprocessed green silicate do not satisfy the universal standard and limits to be used for land reclamation

References

[1] Moustafa, M. I. and Abdelfattah, N. A. Physical and chemical beneficiation of the Egyptian beach monazite. Resource Geol. 60, 288–299 (2010).

[2] Darby, D. A. and Tsang, Y. W. Variation in ilmenite element composition within and among drainage basins: Implications for provenance [J]. *J. Sediment. Petrol*. 87, 831−838 (1987).

[3] Estellita, L., Santos, A. M. A., Anjos, R. M., Yoshimura, E. M., Velasco, H., Da Silva, A. A. R., and Aguiar, J. G. Analysis and risk estimates to workers of Brazilian granitic industries and sandblasters exposed to respirable crystalline silica and natural radionuclides [J]. *Radiation Measurements*. 45, 196−203 (2010).

[4] Shukri, N. M. The mineralogy of some Nile sediments [J]. *Quart. J. Geol. Soc. London*. 105, 511−534 (1950).

[5] Hammoud, N. M. S. Concentration of Monazite from Egyptian Black Sands, Employing Industrial Technique [D]. MSc. Thesis. Fac. Sci. Cairo Univ., Egypt (1966).

[6] Hammoud, N. M. S. Physical and Chemical Properties of Some Egyptian Economic Minerals in Relation to Their Concentration Problems [D]. Fac. Sci. Cairo Univ., Egypt (1973).

[7] Dabbour, G. A. Physical Properties and Distribution of Zircon in Some Egyptian Placer Deposits [D]. MSc. Thesis. Fac. Sci., Cairo Univ., Egypt (1973).

[8] Dabbour, G. A. Geological and Mineralogical Studies on Rutile in the Black Sand Deposits from the Egyptian Mediterranean Coast [D]. Ph. D. Thesis. Fac. Sci., Cairo Univer., Egypt (1980).

[9] Moustafa, M. I. Investigations of Some Physical Properties of Zircon and Rutile to Proper High Purity Mineral Concentrates from Black Sand Deposits, Rosetta, Egypt [D]. MSc. Thesis. Fac. Sci., Mansoura Univer., Egypt (1995).

[10] Moustafa, M. I. Mineralogical and geochemical studies on monazite − Th, REE silicate series in the Egyptian beach monazite concentrate [J]. *J. Sedi. Soc. Egypt*. 17, 63−88 (2009).

[11] Barakat, M. G. Sedimentological Studies and Evaluation of Some Black Sand Deposits on the Northern Coast of Egypt [C]. Fac. Sci., Alexandria Univ., Egypt (2004).

[12] El-Nahas, H. A., Mineralogy, evaluation and upgrading studies on some economic minerals in beach black sands. El Arish area, Egypt. M. Sc. Thesis, Fac. Sci., El Minufiya University, Egypt, 162 p (2002).

[13] Abd El-Wahab, M and El-Nahas, H. A. Radionuclides measurements and mineralogical studies on beach sands, East Rosetta Estuary, Egypt Chin. J. Geochem. 32: 146–156 (2013).

[14] Moustafa, M. I. Mineralogy and beneficiation of some economicminerals in the Egyptian black sands. Ph. D. Thesis, Fac. Sci., Mansoura University, Egypt (1999).

[15] Moustafa, M. I. Separation of economic minerals and discovery of zinc, lead and mercury minerals in the Egyptian black sands. The Third international conference of the geology of africa, Geol. Dept., Fac., Scie., Assuit Univ., Egypt, 153–171 (2003).

[16] Moustafa, M. I. Geochemical studies of the Egyptian beach cassiterite concentrate and its importance as a source of Sn, Ta, Nb and others. The Fifth International Conference on the Geology of Africa, Fac. Sci., Assiut Univ., Assiut, Egypt, 1, 63–78 (2007).

[17] E Elles, P. and Lee, S. Y. Radionuclide-contaminated soil: a mineralogical perspective for their remediation. In: Dixon JB, Schulze DG (eds.) Soil mineralogy with environmental applications, Chap 25. Soil Sci Soc of America, Madison, p 737–763 (2002).

[18] Taboada, T. Cortizas, A. M. Garcı´a, C. Rodeja, E. G. Uranium and thorium in weathering and pedogenetic profiles developed on granitic rocks from NW Spain. Sci Total Environ., 356, 192–206 (2006).

[19] El-Aassy, I. E. Afaf, A. N. El-Galy, M. M., El-Feky, M. G. Abdel Maksoud, T. M., Talaat, Sh. M., Ibrahim, E. M. Behavior and environmental impacts of radionuclides during the hydrometallurgy of calcareous and argillaceous rocks, Southwestern Sinai, Egypt. Appl Radiat and Isotopes. 70, 1024–1033 (2012).

[20] El-Kammar, A. A. Ragab, A. A. Moustafa, M. I. Geochemistry of Economic Heavy Minerals from Rosetta. JAKU: Earth Sci. 22, 69-97 (2011).

[21] Hinton, R. W. and Paterson, B. A. Crystallization history of granitic magma: Evidences from trace elements zoning [J]. *Mineral. Mag*. 58, 416−417 (1994).

[22] Bea, F. Pereira, M. D. Corretage, L. G. Fershtater, G. B. Differentiation of strongly peraluminous, perphosphorous granites: The Pedrobenards Pluton, Central Spain [J]. *Geochimica et Cosmochimica Acta*. 58, 2609−2627 (1994).

[23] Bea, F. Residence of REE, Y, Th and U in granites and crustal protoliths: Implications for the chemistry of crustal melts 11 [J]. *J. Petrol*. 37, 521−552 (1996).

[24] Dabbour, G. A. Mineralogical study on the opaque minerals and secondary rutile from the Egyptian black sands. Proc. Egypt. Academy of Sci., pp. 105–121 (1997).

[25] Lindsley, D. H. Expermintal studies of oxides minerals. Review of Mineralogy. Book Crafters, Inc., Chelsea, Michigan. Vo1. 25, pp. 69-100 (1991).

[26] Large, D. The geology of non-sulphide Zinc Deposits-an overview, Erzmetall 54, 264–276. (2001).

[27] International Atomic Energy Agency (IAEA), Measurement of radionuclides in food and the environment, a guidebook, Technical Reports Series No. 229, Vienna (1989).

[28] Malczewski, D. Taper, L. Dorda, J. Assessment of natural and anthropogenic radioactivity levels in rocks and soils in the environs of Swieradow Zdroj in Sudetes, Poland by in situ gamma-ray spectrometry. J. Environ. Radioact. 73, 233-245 (2004).

[29] El-Galy, M. M. El-Mezayen, A. M. Said, A. F. El Mowafy, A. A. Mohamed, M. S. Distribution and environmental impacts of some radionuclides in sedimentary rocks at Wadi Naseib area, Southwest Sinai, Egypt. Jour. Environ. Radioact. 99, 1075–1082 (2008).

[30] UNSCEAR. United Nations Scientific Committee on the effects of atomic radiation, sources and effects of ionizing radiation. Report to General Assembly, with Scientific Annexes United Nations. United Nations, New York (2000).

[31] Ӧrgün, Y. Altınsoy, N. S. Ahin, S. Y. Gungor, Y. Gultekin, A. H. Karahan, G. Karacık, Z. Natural and anthropogenic radionuclides in rocks and beach sands from Ezine region (Canakkale), Western Anatolia, Turkey. Appl Radiat Isot 65: 739–747 (2007).

[32] Tzortzis, M. Tsertos, H. Christofides, S., Christodoulides, G. Gamma-ray measurements of naturally occurring radioactive samples from Cyprus characteristic geological rocks. Radiat. Meas., 37, 221–229 (2003).

[33] Abbady, A. G. E. Uosif, M. A. M. El-Taher, A. Natural radioactivity and dose assessment for phosphate rocks from Wadi El-Mashash and El-Mahamid Mines, Egypt. Jour. Environ. Radioact., 84, 65–78 (2005).

[34] Beretka, J. and Mathew, P. J. Natural radioactivity of Australian building materials, industrial wastes and by-products [J]. *Health Phys*. 48, 87−95 (1985).

[35] Fares, S. Ashour, A. El-Ashry, M. Abd El-Rahma, M. Gamma Radiation Hazards and Risks Associated with Wastes from Granite Rock Cutting and Polishing Industries in Egypt. Ядерна та радіаційна безпека 1 (53). УДК 539.16: 553.521 (2012).

[36] Anjos, A. M. Veiga, R. Soares, T. Santos, A. M. A. Aguiar, J. G. Frascá, M. H. B. O. Brage, J. A. P. Uzêda, D. Mangia, L. Facure, A. Mosquera, B. Carvalho, C. Gomes, P. R. S. Natural radionuclide distribution in Brazilian commercial granites. Radiation measurements, 39, 245-253 (2005).

[37] Ravisankar, R. Vanasundari, K. Chandrasekaran, A. Rajalakshmi, A. Suganya, M. Vijayagopal, P. Meenakshisundaram, V. Measurement of Natural Radioactivity in Building Materials of Namakkal, Tamil Nadu, India Using Gamma-Ray Spectrometry", Applied Radiation and Isotopes, 70, 699-704 (2012).

[38] EC. European Commission Report on “Radiological Protection Principles concerning the Natural Radioactivity of Building Materials”. Radiation protection 112 (1999).

[39] UNSCEAR. Exposure from natural sources of radiation. Forty-second session of United Nations Scientific Committee on the Effect of Atomic Radiation, Vienna 12-28 May (1993).